Devil's staircase in an optomechanical cavity

Hui Wang, Yuvaraj Dhayalan, and Eyal Buks

Department of Electrical Engineering, Technion, Haifa 32000, Israel

We study self-excited oscillations (SEOs) in an on-fiber optomechanical cavity. While the phase of SEOs randomly diffuses in time when the laser power injected into the cavity is kept constant, phase locking may occur when the laser power is periodically modulated in time. We investigate the dependence of phase locking on the amplitude and frequency of the laser-power modulation. We find that phase locking can be induced with a relatively low modulation amplitude provided that the ratio between the modulation frequency and the frequency of SEOs is tuned close to a rational number of relatively low hierarchy in the Farey tree. To account for the experimental results, a one-dimensional map, which allows evaluating the time evolution of the phase of SEOs, is theoretically derived. By calculating the winding number of the one-dimensional map, the regions of phase locking can be mapped in the plane of modulation amplitude and modulation frequency. Comparison between the theoretical predictions and the experimental findings yields a partial agreement.

Optomechanical cavities [1–7] are widely employed for various sensing [8–11] and photonics [12–18] applications. Moreover, such systems may allow experimental study of the crossover between classical to quantum realms [3,19–28]. The effect of radiation pressure typically governs the optomechanical coupling (i.e., the coupling between the electromagnetic cavity and the mechanical resonator that serves as a movable mirror) when the finesse of the optical cavity is sufficiently high [3,5,23,29–31], whereas bolometric effects can contribute to the optomechanical coupling when optical absorption by the vibrating mirror is significant [4,32–39]. Generally, bolometric effects are dominant in systems consisting of relatively large mirrors, in which the thermal relaxation rate is comparable to the mechanical resonance frequency [36–38,40]. These systems [4,32,34,40–42] exhibit many intriguing phenomena such as mode cooling and self-excited oscillation (SEO) [2,22,34,37,40,43–46]. It has been recently demonstrated that optomechanical cavities can be fabricated on the tip of an optical fiber [47–57]. These micron-scale devices, which can be optically actuated [58], can be used for sensing physical parameters that affect the mechanical properties of the suspended mirror (e.g., absorbed mass, heating by external radiation, acceleration, etc.).

In a recent study [57], phase locking of SEOs has been investigated in an on-fiber optomechanical cavity formed between a fiber Bragg grating (FBG) mirror, serving as a static reflector, and a vibrating mirror, which is fabricated on the tip of a single-mode optical fiber. In that experiment [57] SEOs [8–11] were optically induced by injecting a monochromatic laser light into the on-fiber optomechanical cavity. The optically induced SEO is attributed to the bolometric optomechanical coupling between the optical mode and the mechanical resonator [41,42]. It was found in Ref. [57] that the phase of the SEO can be locked by periodically modulating the laser power that is injected into the cavity. Such phase locking results in entrainment [59–61], i.e., synchronization [62–64] between the SEO and the external modulation [65,66]. Synchronization in self-oscillating systems [63,67–72], in general, can be the result of interaction between systems [73–79], external noise [80–87], or other outside sources,

periodic [88–90] or nonperiodic [91,92]. Synchronization can also be activated by applying a delayed feedback [93–96].

In the experiment reported in Ref. [57], phase locking [97–102] was studied for the case where the ratio between the modulation frequency and the frequency of SEO, which is henceforth labeled as $1 - \alpha$, was tuned close to two values, the first value $1 - \alpha = 1$ corresponds to modulation at the SEO frequency, and the second value $1 - \alpha = 2$ corresponds to modulation at twice the SEO frequency. In the current paper we extend the study and investigate phase locking for arbitrary values of the dimensionless parameter α in the range $[0,1]$. This is done by experimentally mapping the region of phase locking in the plane of the modulation amplitude and modulation frequency. We find that phase locking can be induced with relatively low modulation amplitude provided that α is tuned close to a rational number of relatively low hierarchy in the Farey tree [103]. To account for the experimental results we theoretically evaluate the effect of modulation on the time evolution of the phase of SEO. Some simplifying assumptions and approximations lead to a one-dimensional map [Eq. (5), below], which describes the change that is accumulated over a single period of mechanical oscillation in the relative phase between SEO and the modulation, which is labeled by $2\pi q$. The winding number of the one-dimensional map exhibits a Devil's staircase (Fig. 2, below) [101,104–106], i.e., plateaus near rational values of the parameter α, corresponding to regions where phase locking [99,100] occurs. Partial agreement is obtained from the comparison between the experimental findings and theoretical predictions.

The optomechanical cavity, which is schematically shown in Fig. 1(a), was fabricated on the flat polished tip of a single-mode fused-silica optical fiber with outer diameter of 126 μm (Corning SMF-28 operating at a wavelength band around 1550 nm) held in a zirconia ferrule [56]. A 10-mm-thick chromium layer and a 200 nm gold layer were successively deposited by thermal evaporation. The bilayer was directly patterned by a focused ion beam to the desired mirror shape (20-μm-wide doubly clamped beam). Finally, the mirror was released by etching approximately 12 μm of the underlying silica in 7% HF acid (90 min. etch time at room temperature).
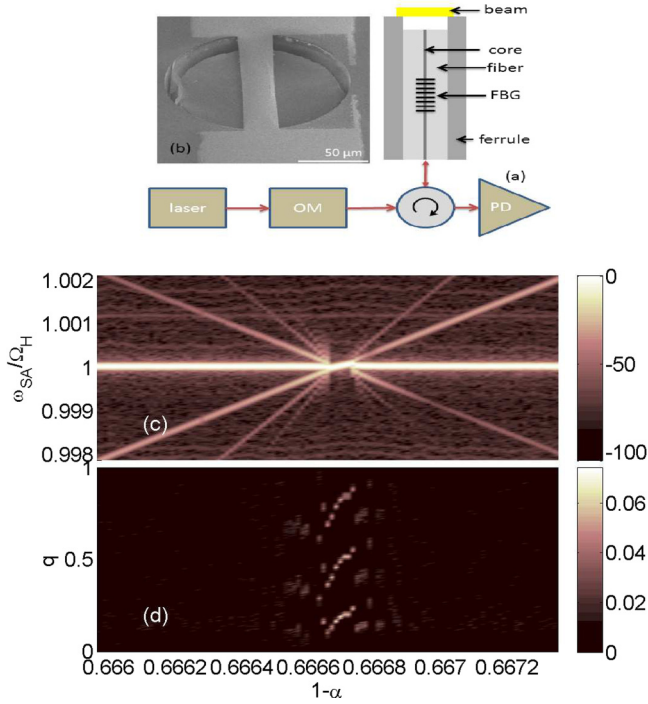
023007-1

FIG. 1. Experimental setup and phase locking. (a) Schematic drawing of the sample and the experimental setup. An on-fiber optomechanical cavity is excited by a tunable laser with external optical modulator (OM). The mechanical resonator has quality factor $Q = \omega_0/(2\gamma_0) = 3800$ and the cavity has finesse $\beta_F = 2.1$. The reflected light intensity is measured by using a photodetector (PD), which is connected to both a spectrum analyzer and an oscilloscope (not shown in the sketch). (b) Electron micrograph of the suspended micromechanical mirror, whose mass is $m = 1.1 \times 10^{-12}$ kg. (c) Spectrum analyzer signal in dB vs $1 - \alpha$ and normalized measurement frequency ω_{SA}/Ω_H. In a region near the point $1 - \alpha = 2/3$, entrainment occurs. The average laser power is set to 12 mW, the wavelength to $\lambda = 1545.498$ nm, and the dimensionless modulation amplitude to $\beta_f = 0.025$. (d) The measured probability distribution $F(q)$ vs $1 - \alpha$. In the same region where entrainment occurs [see panel (c)] the distribution $F(q)$ is peaked near three values [see panel (d)].

The suspended mirror remained supported by the zirconia ferrule, which is resistant to HF.

The static mirror of the optomechanical cavity was provided by a FBG mirror [41] (made by using a standard phase mask technique [107], with grating period of 0.527 μm and length ≈ 8 mm) having a reflectivity band of 0.4 nm full width at half maximum (FWHM) centered at 1545 nm. The length of the optical cavity was $l \approx 10$ mm, providing a free spectral range of $\Delta\lambda = \lambda_0^2/(2n_{eff}l) \approx 80$ pm (where $n_{eff} = 1.468$ is the effective refraction index for SMF-28). Monochromatic light was injected into the fiber bearing the cavity on its tip from a laser source with an adjustable output wavelength λ and power level P_L. The laser was connected through an optical circulator, which allowed the measurement of the reflected light intensity P_R by a fast-responding photodetector [see Fig. 1(a)]. The detected signal was analyzed by an oscilloscope and a spectrum analyzer. The experiments were performed in vacuum (at residual pressure below 0.01 Pa) at a base

temperature of 77 K. The laser power and laser wavelength were first tuned into the regime of SEO before the modulation was turned on.

Phase locking was measured near all fractions $\alpha = n_1/n_2$ in the range $0 < \alpha < 1$, where $n_2 \in \{1,2,3,4,5\}$. The case $1 - \alpha = 2/3$ is demonstrated in Fig. 1. The plot in Fig. 1(c) exhibits the measured signal of a spectrum analyzer, which is connected to the photodetector, vs the normalized modulation frequency $1 - \alpha$ and the normalized measurement frequency ω_{SA}/Ω_H, where $\Omega_H/2\pi = 236.3$ kHz is the frequency of SEO. In the region of phase locking near the point $1 - \alpha = 2/3$ the spectral peak corresponding to SEO coincides with the sideband corresponding to the power modulation. The other spectral lines in Fig. 1(c) converging to the central point $1 - \alpha = 2/3$ and $\omega_{SA}/\Omega_H = 1$ represent higher-order products of frequency mixing between Ω_H and $(1 - \alpha)\Omega_H$ [108]. The plot in Fig. 1(d) exhibits the measured probability distribution $F(q)$ of the variable q, which represents the relative phase between SEO and the modulation in units of 2π. The distribution $F(q)$ is extracted from the oscilloscope's data by employing the zero-crossing technique [109]. While $F(q)$ is found to have a nearly uniform distribution away from the point $1 - \alpha = 2/3$, three pronounced peaks are observed in the region of phase locking near that point, suggesting that the relative phase undergoes a limit cycle of period three.

To account for the experimental findings we theoretically investigate under what conditions phase locking of SEO is expected to occur. In the limit of small displacement, the dynamics of the system can be approximately described by using a single evolution equation [42,110]. The theoretical model that is used to derive the evolution equation [see Eq. (4), below] is briefly described below. Note that some optomechanical effects that were taken into account in the theoretical modeling [42] were found experimentally to have negligible effect on the dynamics [41] (e.g., the effect of radiation pressure). In what follows such effects are disregarded.

The micromechanical mirror in the optical cavity is treated as a mechanical resonator with a single degree of freedom x having mass m and linear damping rate γ_0 (when it is decoupled from the optical cavity). It is assumed that the angular resonance frequency of the mechanical resonator depends on the temperature T of the suspended mirror. For small deviation of T from the base temperature T_0 (i.e., the temperature of the supporting substrate) it is taken to be given by $\omega_0 - \beta T_R$, where $T_R = T - T_0$ and where β is a constant. Furthermore, to model the effect of thermal deformation [34] it is assumed that a temperature-dependent force given by $m\theta T_R$, where θ is a constant, acts on the mechanical resonator [39]. When noise is disregarded, the equation of motion governing the dynamics of the mechanical resonator is taken to be given by

$$\frac{d^2x}{dt^2} + 2\gamma_0 \frac{dx}{dt} + (\omega_0 - \beta T_R)^2 x = \theta T_R. \tag{1}$$

The intracavity optical power incident on the suspended mirror is denoted by $P_L I(x)$, where P_L is the injected laser power, and the function $I(x)$ depends on the mechanical displacement x [see Eq. (3), below]. The time evolution of the relative temperature T_R is governed by the thermal balance

equation

$$\frac{dT_{\mathrm{R}}}{dt} = Q - \kappa T_{\mathrm{R}},\tag{2}$$

where $Q = \eta P_{\mathrm{L}} I(x)$ is proportional to the heating power, η is the heating coefficient due to optical absorption, and κ is the thermal decay rate.

The function $I(x)$ depends on the properties of the optical cavity that is formed between the suspended mechanical mirror and the on-fiber static reflector. The finesse of the optical cavity is limited by loss mechanisms that give rise to optical energy leaking out of the cavity. The main escape routes are through the on-fiber static reflector, through absorption by the metallic mirror, and through radiation. The corresponding transmission probabilities are respectively denoted by $\mathcal{T}_{\mathrm{B}}$, $\mathcal{T}_{\mathrm{A}}$, and $\mathcal{T}_{\mathrm{R}}$. In terms of these parameters, the function $I(x)$ is given by [41]

$$I(x) = \frac{\beta_{\mathrm{F}}\left(1 - \frac{\beta_-^2}{\beta_+^2}\right)\beta_+^2}{1 - \cos\frac{4\pi x_{\mathrm{D}}}{\lambda} + \beta_+^2},\tag{3}$$

where $x_{\mathrm{D}} = x - x_{\mathrm{R}}$ is the displacement of the mirror relative to a point x_{R}, at which the energy stored in the optical cavity in steady state obtains a local maximum, $\beta_\pm^2 = (\mathcal{T}_{\mathrm{B}} \pm \mathcal{T}_{\mathrm{A}} \pm \mathcal{T}_{\mathrm{R}})^2/8$ and where β_{F} is the cavity finesse. The reflection probability $R_{\mathrm{C}} = P_{\mathrm{R}}/P_{\mathrm{L}}$ is given in steady state by [41,111] $R_{\mathrm{C}} = 1 - I(x)/\beta_{\mathrm{F}}$. For sufficiently small x, the expansion $I(x) = I_0 + I_0'x + (1/2)I_0''x^2 + O(x^3)$ can be employed, where a prime denotes differentiation with respect to the displacement x.

Consider the case where the laser power P_{L} is modulated in time according to $P_{\mathrm{L}}(t) = P_0 + P_1(t)$, where P_0 is a constant and $P_1(t)$ is assumed to have a vanishing average. When both P_1 and $I - I_0$ are sufficiently small, the problem can be significantly simplified by employing the approximation $Q \simeq \eta P_0 I + \eta P_1 I_0$. The displacement $x(t)$ is expressed in terms of the complex amplitude A as $x(t) = x_0 + 2\,\mathrm{Re}\,A$, where x_0, which is given by $x_0 = \eta\theta P_0 I_0/(\kappa\omega_0^2)$, is the averaged optically induced static displacement. For a small displacement, the evolution equation for the complex
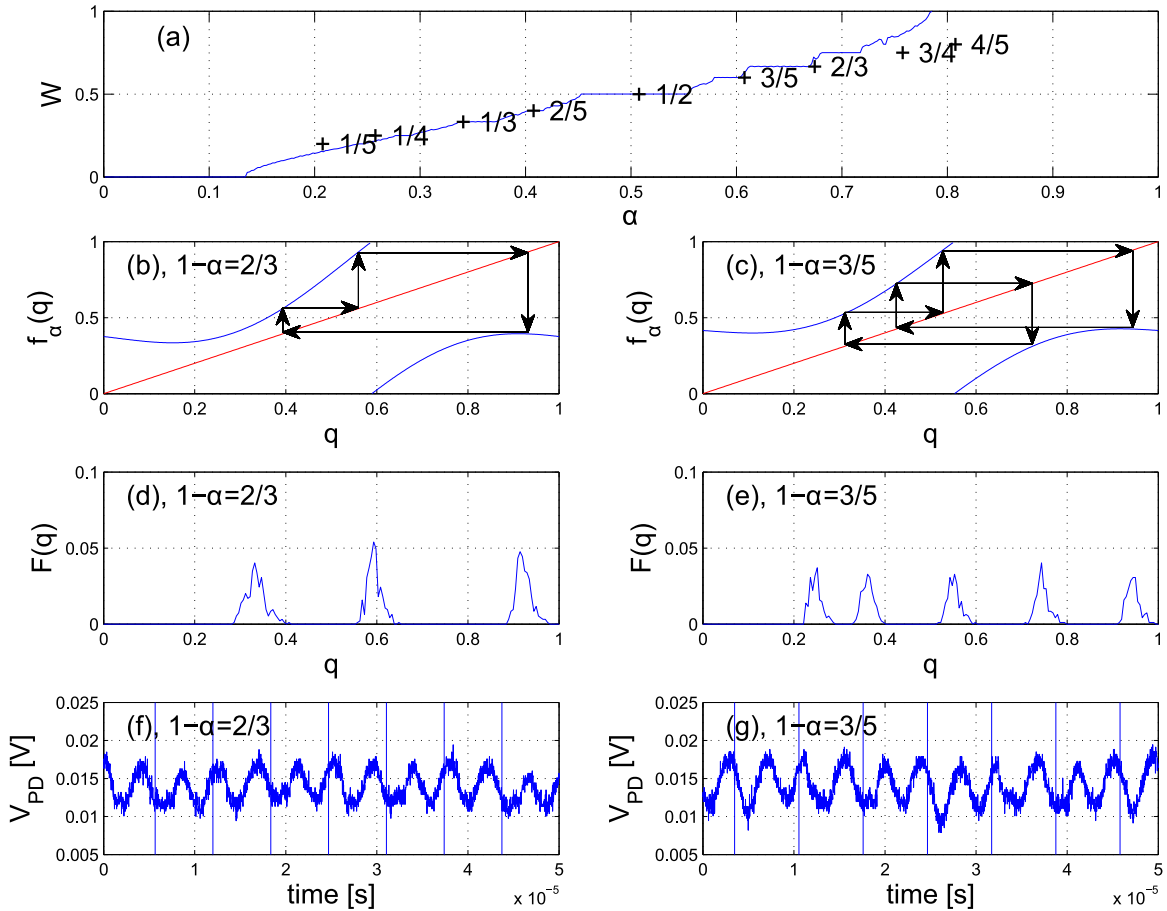

FIG. 2. The winding number and limit cycles. (a) Devil's staircase in the plot of the winding number W vs α for the case where $\beta_{\mathrm{f}} = 0.0355$. Locally stable limit cycles for the case $1 - \alpha = 2/3$ and $\beta_{\mathrm{f}} = 0.025$ are presented in panels (b), (d), and (f) and for the case $1 - \alpha = 3/5$ and $\beta_{\mathrm{f}} = 0.028$ in panels (c), (e), and (g). The map $f_\alpha(q)$ together with the corresponding limit cycle for the case $1 - \alpha = 2/3$ ($1 - \alpha = 3/5$) is depicted in panel (b) [panel (c)], the experimentally measured probability distribution $F(q)$ in panel (d) [panel (e)], and a sample temporal data in panel (f) [panel (g)] (the vertical lines label the beginning points of each modulation period). In the experimental measurements presented in this plot a pulse-power modulation having a rectangular (instead of a sinusoidal) waveform has been employed. For that case, the recursive relation $q_{n+1} = f_\alpha(q_n)$ is derived by first performing a Fourier decomposition of the rectangular waveform, and then calculating the contribution of each Fourier component by using Eq. (6).

amplitude A is found to be given by [42,57]

$$\dot{A} + (\Gamma_{\text{eff}} + i\Omega_{\text{eff}})A = \xi(t) + \vartheta(t), \quad (4)$$

where both the effective resonance frequency Ω_{eff} and the effective damping rate Γ_{eff} are real even functions of $|A|$. To second order in $|A|$ they are given by $\Gamma_{\text{eff}} = \Gamma_0 + \Gamma_2|A|^2$ and $\Omega_{\text{eff}} = \Omega_0 + \Omega_2|A|^2$, where $\Gamma_0 = \gamma_0 + \eta\theta P_1 I_0'/(2\omega_0^2)$, $\Gamma_2 = \gamma_2 + \eta\beta P_1 I_0''/(4\omega_0)$, with γ_2 being the intrinsic mechanical nonlinear quadratic damping rate [112], $\Omega_0 = \omega_0 - \eta\beta P_1 I_0/\kappa$, and $\Omega_2 = -\eta\beta P_1 I_0''/\kappa$. Note that the above expressions for Γ_{eff} and Ω_{eff} are obtained by making the following assumptions: $\kappa^2/(\omega_0^3\lambda) \ll \beta/\theta \ll 1/(2\omega_0 x_0)$ and $\kappa \ll \omega_0$, both typically hold experimentally [41]. The term $\xi(t)$, which is given by $\xi(t) = \Omega_0^{-1}\theta T_{\text{R1}}(t)$, where $T_{\text{R1}}(t)$ is found by solving Eq. (2) for the case where the the laser power is taken to be $P_1(t)$, represents the thermal force that is generated due to the power modulation. The fluctuating term [113,114] $\vartheta(t) = \vartheta_x(t) + i\vartheta_y(t)$, where both ϑ_x and ϑ_y are real, represents white noise and the following is assumed to hold: $\langle\vartheta_x(t)\vartheta_x(t')\rangle = \langle\vartheta_y(t)\vartheta_y(t')\rangle = 2\Theta\delta(t - t')$ and $\langle\vartheta_x(t)\vartheta_y(t')\rangle = 0$, where $\Theta = \gamma_0 k_B T_{\text{eff}}/(4m\omega_0^2)$, k_B is Boltzmann's constant, and T_{eff} is the effective noise temperature.

In the absence of laser modulation, i.e., when $P_1 = 0$, the equation of motion (4) describes a van der Pol oscillator [98]. Consider the case where $\Gamma_2 > 0$, for which a supercritical Hopf bifurcation occurs when the linear damping coefficient Γ_0 vanishes. Above threshold, i.e., when Γ_0 becomes negative, the amplitude $A_r = |A|$ of SEOs is given by $A_{r0} = \sqrt{-\Gamma_0/\Gamma_2}$ and the angular frequency Ω_H of SEOs by $\Omega_H = \Omega_{\text{eff}}(A_{r0})$. For our experimental parameters $|\Omega_2| \ll \omega_0/A_{r0}^2$, and consequently to a good approximation the dependence of Ω_H on A_{r0} can be disregarded.

The laser-power modulation $P_1(t)$ is taken to be time periodic with angular frequency $(1 - \alpha)\Omega_H$, a sinusoidal waveform and an amplitude P_p, which is expressed as $P_p = \beta_f\Omega_H^3 A_{r0}/(\theta\eta I_0)$, where both α and β_f are real dimensionless constants. Let $2\pi q_n$ be the relative phase of SEO with respect to the external modulation after an integer number n of periods of mechanical oscillation. Integrating Eq. (4) over a single period of SEO (and disregarding the noise term) yields for the case where $\beta_f \ll 1$ a recursive relation between q_{n+1} and q_n which reads

$$q_{n+1} = f_\alpha(q_n), \quad (5)$$

where

$$f_\alpha(q) = q + \alpha + \frac{2\beta_f \sin(\pi\alpha)\cos(\pi\alpha + 2\pi q)}{(1 - \alpha)[1 - (1 - \alpha)^2]}. \quad (6)$$

The winding number W is defined by [101]

$$W = \lim_{n\to\infty} \frac{q_{n+1} - q_1}{n}. \quad (7)$$

For the case of a limit cycle, the winding number is a rational number given by $W = n_1/n_2$, where n_2 is the period of the cycle and n_1 is the number of sweeps through the unit interval $[0,1]$ in a cycle when the mapping (6) is considered as modulo 1. The Devil's staircase can be seen in Fig. 2(a), in which the winding number W is plotted as a function of α for the case where $\beta_f = 0.0355$. Locally stable limit cycles are

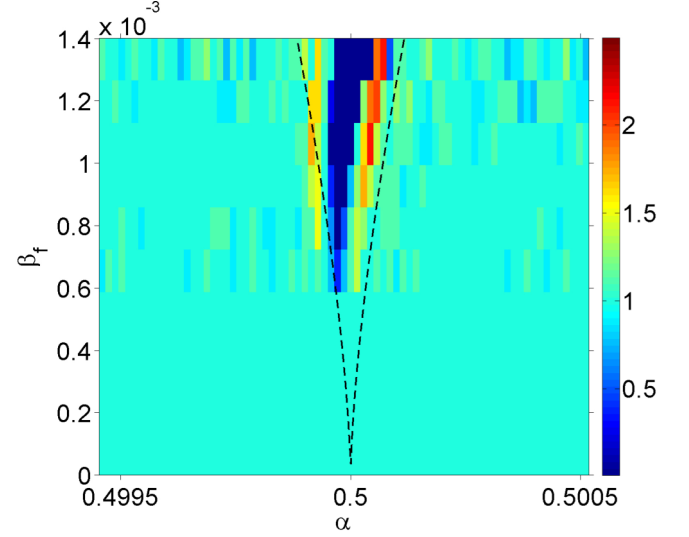

FIG. 3. Arnold tongue near the point $\alpha = 1/2$. The color map represents the measured value of the derivative $dW/d\alpha$ vs α and β_f. The black dotted line represents the theoretically calculated bifurcation line $\beta_f = (81/128\pi)^{1/3}(\alpha - 1/2)^{2/3}$. Laser parameters are the same as those listed in the caption of Fig. 1. The experimental value of the dimensionless parameter β_f is determined by using the following device parameter: $\Omega_H^3 A_{r0}/(\theta\eta I_0) = 0.10$ W.

presented in Fig. 2 for the case $1 - \alpha = 2/3$ and $\beta_f = 0.025$ [Figs. 2(b), 2(d), and 2(f)] and for the case $1 - \alpha = 3/5$ and $\beta_f = 0.028$ [Figs. 2(c), 2(e), and 2(g)]. The map $f_\alpha(q)$ together with the corresponding limit cycle for the case $1 - \alpha = 2/3$ ($1 - \alpha = 3/5$) is depicted in Fig. 2(b) [Fig. 2(c)], the experimentally measured probability distribution $F(q)$ in Fig. 2(d) [Fig. 2(e)], and a sample of temporal data in Fig. 2(f) [Fig. 2(g)]. The comparison between the values of q corresponding to the peaks in the measured distribution $F(q)$ [Figs. 2(d) and 2(e)] and the values of q corresponding to the calculated limit cycle [Figs. 2(b) and 2(c)] exhibits a partial agreement.

Regions of phase locking in the plane that is spanned by the modulation parameters (frequency and amplitude) are commonly called Arnold tongues. The Arnold tongue near $\alpha = 1/2$ is seen in Fig. 3. The color map exhibits the measured value of the derivative $dW/d\alpha$ vs α and β_f. Near the point $\alpha = 1/2$ the Arnold tongue (the region where $dW/d\alpha \simeq 0$ in Fig. 3) represents the stability zone of a fixed point of the second-order map $\mathcal{F}_{2,\alpha}(q) \equiv f_\alpha(f_\alpha(q))$. To account for the experimental results, the behavior of the map $\mathcal{F}_{2,\alpha}(q)$ is theoretically investigated near the point $\alpha = 1/2$. By expressing α as $\alpha = 1/2 + \epsilon$ and by expanding $\mathcal{F}_{2,\alpha}(q)$ up to first order in ϵ, the fixed point, which is labeled q_f, can be analytically evaluated to lowest nonvanishing order in β_f. The region of stability, which is found from the requirement that $|\mathcal{F}'_{2,\alpha}(q_f)| < 1$, yields the bifurcation line in the plane spanned by α and β_f, which is found to be given by $\beta_f = (81/128\pi)^{1/3}\epsilon^{2/3}$ (see the black dotted line in Fig. 3). The comparison between data and theory yields a moderate agreement.

In summary, the Devil's staircase in an on-fiber optomechanical cavity is investigated. The device under study can

be employed as a sensor operating in the region of SEO. Future study will address the possibility of reducing phase noise by inducing phase locking in order to enhance sensor's performance.

[1] V. Braginsky and A. Manukin, Ponderomotive effects of electromagnetic radiation, Sov. Phys. JETP **25**, 653 (1967).

[2] K. Hane and K. Suzuki, Self-excited vibration of a self-supporting thin film caused by laser irradiation, Sens. Actuators, A **51**, 179 (1996).

[3] S. Gigan, H. R. Böhm, M. Paternostro, F. Blaser, J. B. Hertzberg, K. C. Schwab, D. Bauerle, M. Aspelmeyer, and A. Zeilinger, Self cooling of a micromirror by radiation pressure, Nature (London) **444**, 67 (2006).

[4] C. H. Metzger and K. Karrai, Cavity cooling of a microlever, Nature (London) **432**, 1002 (2004).

[5] T. J. Kippenberg and K. J. Vahala, Cavity optomechanics: Back-action at the mesoscale, Science **321**, 1172 (2008).

[6] C. Metzger I. Favero, S. Camerer, D. Konig, H. Lorenz, J. P. Kotthaus, and K. Karrai, Optical cooling of a micromirror of wavelength size, Appl. Phys. Lett. **90**, 104101 (2007).

[7] F. Marquardt and S. M. Girvin, Optomechanics, Physics **2**, 40 (2009).

[8] D. Rugar, H. J. Mamin, and P. Guethner, Improved fiber-optic interferometer for atomic force microscopy, Appl. Phys. Lett. **55**, 2588 (1989).

[9] O. Arcizet, P.-F. Cohadon, T. Briant, M. Pinard, A. Heidmann, J.-M. Mackowski, C. Michel, L. Pinard, O. Français, and L. Rousseau, High-Sensitivity Optical Monitoring of a Micromechanical Resonator with a Quantum-Limited Optomechanical Sensor, Phys. Rev. Lett. **97**, 133601 (2006).

[10] S. Forstner, S. Prams, J. Knittel, E. D. van Ooijen, J. D. Swaim, G. I. Harris, A. Szorkovszky, W. P. Bowen, and H. Rubinsztein-Dunlop, Cavity Optomechanical Magnetometer, Phys. Rev. Lett. **108**, 120801 (2012).

[11] S. Stapfner, L. Ost, D. Hunger, J. Reichel, I. Favero, and E. M. Weig, Cavity-enhanced optical detection of carbon nanotube Brownian motion, Appl. Phys. Lett. **102**, 151910 (2013).

[12] S. E. Lyshevski and M. A. Lyshevski, Nano- and micro-optoelectromechanical systems and nanoscale active optics, in *Proceedings of the Third IEEE Conference on Nanotechnology* (IEEE, New York, 2003), Vol. 2, pp. 840–843.

[13] N. A. D. Stokes, F. M. A. Fatah, and S. Venkatesh, Self-excited vibrations of optical microresonators, Electron. Lett. **24**, 777 (1988).

[14] M. Hossein-Zadeh and K. J. Vahala, An optomechanical oscillator on a silicon chip, IEEE J. Sel. Top. Quantum Electron. **16**, 276 (2010).

[15] M. C. Wu, O. Solgaard, and J. E. Ford, Optical MEMS for lightwave communication, J. Lightwave Technol. **24**, 4433 (2006).

[16] M. Eichenfield, C. P. Michael, R. Perahia, and O. Painter, Actuation of micro-optomechanical systems via cavity-enhanced optical dipole forces, Nat. Photon. **1**, 416 (2007).

[17] G. Bahl, J. Zehnpfennig, M. Tomes, and T. Carmon, Stimulated optomechanical excitation of surface acoustic waves in a microdevice, Nat. Commun. **2**, 403 (2011).

[18] N. E. Flowers-Jacobs, S. W. Hoch, J. C. Sankey, A. Kashkanova, A. M. Jayich, C. Deutsch, J. Reichel, and J. G. E. Harris, Fiber-cavity-based optomechanical device, Appl. Phys. Lett. **101**, 221109 (2012).

[19] J. D. Thompson, B. M. Zwickl, A. M. Jayich, F. Marquardt, S. M. Girvin, and J. G. E. Harris, Strong dispersive coupling of a high-finesse cavity to a micromechanical membrane, Nature (London) **452**, 72 (2008).

[20] Pierre Meystre, A short walk through quantum optomechanics, Ann. Phys. (Berlin, Ger.) **525**, 215 (2013).

[21] H. J. Kimble, Y. Levin, A. B. Matsko, K. S. Thorne, and S. P. Vyatchanin, Conversion of conventional gravitational-wave interferometers into quantum nondemolition interferometers by modifying their input and/or output optics, Phys. Rev. D **65**, 022002 (2001).

[22] T. Carmon, H. Rokhsari, L. Yang, T. J. Kippenberg, and K. J. Vahala, Temporal Behavior of Radiation-Pressure-Induced Vibrations of an Optical Microcavity Phonon Mode, Phys. Rev. Lett. **94**, 223902 (2005).

[23] O. Arcizet, P. F. Cohadon, T. Briant, M. Pinard, and A. Heidmann, Radiation-pressure cooling and optomechanical instability of a micromirror, Nature (London) **444**, 71 (2006).

[24] A. M. Jayich, J. C. Sankey, B. M. Zwickl, C. Yang, J. D. Thompson, S. M. Girvin, A. A. Clerk, F. Marquardt, and J. G. E. Harris, Dispersive optomechanics: A membrane inside a cavity, New J. Phys. **10**, 095008 (2008).

[25] A. Schliesser, R. Riviere, G. Anetsberger, O. Arcizet, and T. J. Kippenberg, Resolved-sideband cooling of a micromechanical oscillator, Nat. Phys. **4**, 415 (2008).

[26] C. Genes, D. Vitali, P. Tombesi, S. Gigan, and M. Aspelmeyer, Ground-state cooling of a micromechanical oscillator: Comparing cold damping and cavity-assisted cooling schemes, Phys. Rev. A **77**, 033804 (2008).

[27] J. D. Teufel, D. Li, M. S. Allman, K. Cicak, A. J. Sirois, J. D. Whittaker, and R. W. Simmonds, Circuit cavity electromechanics in the strong-coupling regime, Nature (London) **471**, 204 (2011).

[28] M. Poot and H. S. J. van der Zant, Mechanical systems in the quantum regime, Phys. Rep. **511**, 273 (2012).

[29] T. J. Kippenberg, H. Rokhsari, T. Carmon, A. Scherer, and K. J. Vahala, Analysis of Radiation-Pressure Induced Mechanical Oscillation of an Optical Microcavity, Phys. Rev. Lett. **95**, 033901 (2005).

[30] H. Rokhsari, T. Kippenberg, T. Carmon, and K. J. Vahala, Radiation-pressure-driven micro-mechanical oscillator, Opt. Express **13**, 5293 (2005).

[31] D. Kleckner and D. Bouwmeester, Sub-kelvin optical cooling of a micromechanical resonator, Nature (London) **444**, 75 (2006).

[32] G. Jourdan, F. Comin, and J. Chevrier, Mechanical Mode Dependence of Bolometric Backaction in an Atomic Force Microscopy Microlever, Phys. Rev. Lett. **101**, 133904 (2008).

[33] F. Marino and F. Marin, Chaotically spiking attractors in suspended-mirror optical cavities, Phys. Rev. E **83**, 015202 (2011).

[34] C. Metzger, M. Ludwig, C. Neuenhahn, A. Ortlieb, I. Favero, K. Karrai, and F. Marquardt, Self-Induced Oscillations in an Optomechanical System Driven by Bolometric Backaction, Phys. Rev. Lett. **101**, 133903 (2008).

[35] J. Restrepo, J. Gabelli, C. Ciuti, and I. Favero, Classical and quantum theory of photothermal cavity cooling of a mechanical oscillator, C. R. Phys. **12**, 860 (2011).

[36] S. D. Liberato, N. Lambert, and F. Nori, Quantum noise in photothermal cooling, Phys. Rev. A **83**, 033809 (2011).

[37] F. Marquardt, J. G. E. Harris, and S. M. Girvin, Dynamical Multistability Induced by Radiation Pressure in High-Finesse Micromechanical Optical Cavities, Phys. Rev. Lett. **96**, 103901 (2006).

[38] M. Paternostro, S. Gigan, M. S. Kim, F. Blaser, H. R. Böhm, and M. Aspelmeyer, Reconstructing the dynamics of a movable mirror in a detuned optical cavity, New J. Phys. **8**, 107 (2006).

[39] D. Yuvaraj, M. B. Kadam, O. Shtempluck, and E. Buks, Optomechanical cavity with a buckled mirror, J. Microelectromech. Syst. **22**, 430 (2013).

[40] K. Aubin, M. Zalalutdinov, T. Alan, R. B. Reichenbach, R. Rand, A. Zehnder, J. Parpia, and H. Craighead, Limit cycle oscillations in CW laser-driven NEMS, J. Microelectromech. Syst. **13**, 1018 (2004).

[41] S. Zaitsev, A. K. Pandey, O. Shtempluck, and E. Buks, Forced and self-excited oscillations of optomechanical cavity, Phys. Rev. E **84**, 046605 (2011).

[42] S. Zaitsev, O. Gottlieb, and E. Buks, Nonlinear dynamics of a microelectromechanical mirror in an optical resonance cavity, Nonlinear Dyn. **69**, 1589 (2012).

[43] K. Kim and S. Lee, Self-oscillation mode induced in an atomic force microscope cantilever, J. Appl. Phys. **91**, 4715 (2002).

[44] T. Corbitt, D. Ottaway, E. Innerhofer, J. Pelc, and N. Mavalvala, Measurement of radiation-pressure-induced optomechanical dynamics in a suspended Fabry-Perot cavity, Phys. Rev. A **74**, 021802 (2006).

[45] T. Carmon and K. J. Vahala, Modal Spectroscopy of Optoexcited Vibrations of a Micron-Scale on-Chip Resonator at Greater than 1 GHz Frequency, Phys. Rev. Lett. **98**, 123901 (2007).

[46] M. Bagheri, M. Poot, M. Li, W. P. H. Pernice, and H. X. Tang, Dynamic manipulation of nanomechanical resonators in the high-amplitude regime and non-volatile mechanical memory operation, Nat. Nanotechnol. **6**, 726 (2011).

[47] D. Iannuzzi, S. Deladi, V. J. Gadgil, R. G. P. Sanders, H. Schreuders, and M. C. Elwenspoek, Monolithic fiber-top sensor for critical environments and standard applications, Appl. Phys. Lett. **88**, 053501 (2006).

[48] C. Ma and A. Wang, Optical fiber tip acoustic resonator for hydrogen sensing, Opt. Lett. **35**, 2043 (2010).

[49] D. Chavan, G. Gruca, S. de Man, M. Slaman, J. H. Rector, K. Heeck, and D. Iannuzzi, Ferrule-top atomic force microscope, Rev. Sci. Instrum. **81**, 123702 (2010).

[50] K. B. Gavan, J. H. Rector, K. Heeck, D. Chavan, G. Gruca, T. H. Oosterkamp, and D. Iannuzzi, Top-down approach to fiber-top cantilevers, Opt. Lett. **36**, 2898 (2011).

[51] I. W. Jung, B. Park, J. Provine, R. T. Howe, and O. Solgaard, Highly sensitive monolithic silicon photonic crystal fiber tip sensor for simultaneous measurement of refractive index and temperature, J. Lightwave Technol. **29**, 1367 (2011).

[52] A. Butsch, M. S. Kang, T. G. Euser, J. R. Koehler, S. Rammler, R. Keding, and P. St. J. Russell, Optomechanical Nonlinearity in Dual-Nanoweb Structure Suspended Inside Capillary Fiber, Phys. Rev. Lett. **109**, 183904 (2012).

[53] F. Albri, J. Li, R. R. J. Maier, W. N. MacPherson, and D. P. Hand, Laser machining of sensing components on the end of optical fibres, J. Micromech. Microeng. **23**, 045021 (2013).

[54] A. B. Shkarin, N. E. Flowers-Jacobs, S. W. Hoch, A. D. Kashkanova, C. Deutsch, J. Reichel, and J. G. E. Harris, Optically Mediated Hybridization Between Two Mechanical Modes, Phys. Rev. Lett. **112**, 013602 (2014).

[55] I. Baskin, D. Yuvaraj, G. Bachar, K. Shlomi, O. Shtempluck, and E. Buks, Optically induced self-excited oscillations in an on-fiber optomechanical cavity, J. Microelectromech. Syst. **23**, 563 (2014).

[56] Y. Dhayalan, I. Baskin, K. Shlomi, and E. Buks, Phase Space Distribution Near the Self-Excited Oscillation Threshold, Phys. Rev. Lett. **112**, 210403 (2014).

[57] K. Shlomi, D. Yuvaraj, I. Baskin, O. Suchoi, R. Winik, and E. Buks, Synchronization in an optomechanical cavity, Phys. Rev. E **91**, 032910 (2015).

[58] G. Gruca, D. Chavan, J. Rector, K. Heeck, and D. Iannuzzi, Demonstration of an optically actuated ferrule-top device for pressure and humidity sensing, Sens. Actuators, A **190**, 77 (2013).

[59] R. Hamerly and H. Mabuchi, Optical Devices Based on Limit Cycles and Amplification in Semiconductor Optical Cavities, Phys. Rev. Applied **4**, 024016 (2015).

[60] D. B. Blocher, A. T. Zehnder, and R. H. Rand, Entrainment of micromechanical limit cycle oscillators in the presence of frequency instability, J. Microelectromech. Syst. **22**, 835 (2013).

[61] L. G. Villanueva, E. Kenig, R. B. Karabalin, M. H. Matheny, Ron Lifshitz, M. C. Cross, and M. L. Roukes, Surpassing Fundamental Limits of Oscillators Using Nonlinear Resonators, Phys. Rev. Lett. **110**, 177208 (2013).

[62] C. Huygens and H. Oscillatorium, *The Pendulum Clock*, Trans. R. J. Blackwell (The Iowa State University Press, Ames, 1986).

[63] M. Rosenblum and A. Pikovsky, Synchronization: from pendulum clocks to chaotic lasers and chemical oscillators, Contemp. Phys. **44**, 401 (2003).

[64] M. C. Cross, A. Zumdieck, R. Lifshitz, and J. L. Rogers, Synchronization by Nonlinear Frequency Pulling, Phys. Rev. Lett. **93**, 224101 (2004).

[65] G. Heinrich, M. Ludwig, J. Qian, B. Kubala, and F. Marquardt, Collective Dynamics in Optomechanical Arrays, Phys. Rev. Lett. **107**, 043603 (2011).

[66] S. Y. Shah, M. Zhang, R. Rand, and M. Lipson, Master-Slave Locking of Optomechanical Oscillators Over a Long Distance, Phys. Rev. Lett. **114**, 113602 (2015).

[67] G. V. Osipov, J. Kurths, and C. Zhou, *Synchronization in Oscillatory Networks* (Springer, New York, 2007).

[68] A. Pikovsky, M. Rosenblum, and J. Kurths, Phase synchronization in regular and chaotic systems, Int. J. Bifurcation Chaos Appl. Sci. Eng. **10**, 2291 (2000).

[69] V. S. Afraimovich, V. I. Nekorkin, G. V. Osipov, and A. V. Gaponov-Grekhov, *Stability, Structures and Chaos in*

Nonlinear Synchronization Networks (World Scientific, Singapore, 1994).

[70] Yu. I. Kuznetsov, P. S. Landa, A. F. Ol'Khovoi, and S. M. Perminov, Relationship between the amplitude threshold of synchronization and the entropy in stochastic self-excited systems, Sov. Phys. Doklady **30**, 221 (1985).

[71] P. S. Landa, *Regular and Chaotic Oscillations* (Springer, New York, 2001).

[72] A. L. Fradkov and A. Yu. Pogromsky, *Introduction to Control of Oscillations and Chaos* (World Scientific, Singapore, 1998), Vol 35.

[73] L. M. Pecora and T. L. Carroll, Driving systems with chaotic signals, Phys. Rev. A **44**, 2374 (1991).

[74] L. M. Pecora and T. L. Carroll, Synchronization in Chaotic Systems, Phys. Rev. Lett. **64**, 821 (1990).

[75] M. de Sousa Vieira, A. J. Lichtenberg, and M. A. Lieberman, Synchronization of regular and chaotic systems, Phys. Rev. A **46**, R7359 (1992).

[76] H. Fujisaka and T. Yamada, Stability theory of synchronized motion in coupled-oscillator systems, Prog. Theor. Phys. **69**, 32 (1983).

[77] P. S. Landa and M. G. Rosenblum, Synchronization and chaotization of oscillations in coupled self-oscillating systems, Appl. Mech. Rev. **46**, 414 (1993).

[78] J. Warminski, Nonlinear normal modes of a self-excited system driven by parametric and external excitations, Nonlinear Dyn. **61**, 677 (2010).

[79] M.-A. Lemonde, N. Didier, and A. A. Clerk, Nonlinear Interaction Effects in a Strongly Driven Optomechanical Cavity, Phys. Rev. Lett. **111**, 053602 (2013).

[80] A. S. Pikovsky, Synchronization and stochastization of the ensemble of autogenerators by external noise, Radiophys. Quantum Electron. **27**, 576 (1984).

[81] A. G. Balanov, N. B. Janson, and P. V. E. McClintock, Coherence resonance of the noise-induced motion on the way to breakdown of synchronization in chaotic systems, Fluct. Noise Lett. **3**, L113 (2003).

[82] K. Czołczynski, P. Perlikowski, A. Stefański, and T. Kapitaniak, Synchronization of self-excited oscillators suspended on elastic structure, Chaos, Solitons Fractals **32**, 937 (2007).

[83] A. G. Balanov, N. B. Janson, D. E. Postnov, and P. V. E. McClintock, Coherence resonance versus synchronization in a periodically forced self-sustained system, Phys. Rev. E **65**, 041105 (2002).

[84] X.-J. Zhang and G.-X. Wang, Stochastic resonance and signal recovery in two-dimensional arrays of coupled oscillators, Physica A (Amsterdam, Neth.) **345**, 411 (2005).

[85] M. G. Rosenblum, A. S. Pikovsky, and J. Kurths, Phase Synchronization of Chaotic Oscillators, Phys. Rev. Lett. **76**, 1804 (1996).

[86] A. S. Pikovsky, M. G. Rosenblum, G. V. Osipov, and J. Kurths, Phase synchronization of chaotic oscillators by external driving, Physica D **104**, 219 (1997).

[87] Y. T. Yang, C. Callegari, X. L. Feng, and M. L. Roukes, Surface adsorbate fluctuations and noise in nanoelectromechanical systems, Nano Lett. **11**, 1753 (2011).

[88] A. A. Koronovskii, M. K. Kurovskaya, and A. E. Hramov, Relationship between phase synchronization of chaotic oscillators and time scale synchronization, Tech. Phys. Lett. **31**, 847 (2005).

[89] A. P. Nikitin and N. G. Stocks, Estimation of periodicity in synchronised systems, in *Second International Symposium on Fluctuations and Noise* (International Society for Optics and Photonics, 2004), p. 171.

[90] M. Qian and X.-J. Zhang, Frequency resonance in stochastic systems, Chin. Phys. Lett. **20**, 202 (2003).

[91] S. Nakabayashi and K. Uosaki, Synchronization of electrochemical oscillations with external perturbations, Chem. Phys. Lett. **217**, 163 (1994).

[92] M. G. Rosenblum, A. S. Pikovsky, J. Kurths, G. V. Osipov, I. Z. Kiss, and J. L. Hudson, Locking-Based Frequency Measurement and Synchronization of Chaotic Oscillators with Complex Dynamics, Phys. Rev. Lett. **89**, 264102 (2002).

[93] N. B. Janson, A. G. Balanov, and E. Schöll, Delayed Feedback as a Means of Control of Noise-Induced Motion, Phys. Rev. Lett. **93**, 010601 (2004).

[94] A. G. Balanov, N. B. Janson, and E. Schöll, Control of noise-induced oscillations by delayed feedback, Physica D **199**, 1 (2004).

[95] E. Schöll, A. G. Balanov, N. B. Janson, and A. Neiman, Controlling stochastic oscillations close to a Hopf bifurcation by time-delayed feedback, Stoch. Dynam. **5**, 281 (2005).

[96] M. Hamdi and M. Belhaq, Quasi-periodic oscillation envelopes and frequency locking in rapidly vibrated nonlinear systems with time delay, Nonlinear Dynam. **73**, 1 (2013).

[97] V. S. Anishchenko and T. E. Vadivasova, Synchronization of self-oscillations and noise-induced oscillations, J. Commun. Technol. Electron. **47**, 117 (2002).

[98] M. Pandey, R. H. Rand, and A. T. Zehnder, Frequency locking in a forced Mathieu–van der Pol–Duffing system, Nonlinear Dyn. **54**, 3 (2008).

[99] L. J. Paciorek, Injection locking of oscillators, Proc. IEEE **53**, 1723 (1996).

[100] R. Adler, A study of locking phenomena in oscillators, Proc. IRE **34**, 351 (1946).

[101] M. Høgh Jensen, P. Bak, and T. Bohr, Complete Devil's Staircase, Fractal Dimension, and Universality of Mode-Locking Structure in the Circle Map, Phys. Rev. Lett. **50**, 1637 (1983).

[102] S. Dos Santos and M. Planat, Generation of $1/f$ noise in locked systems working in nonlinear mode, IEEE Trans. Ultrson. Ferroelectr. Freq. Control **47**, 1147 (2000).

[103] J. Glazier, A. Libchaber *et al.*, Quasi-periodicity and dynamical systems: an experimentalist's view, IEEE Trans. Circuits Syst. **35**, 790 (1988).

[104] E. Ben-Jacob, Y. Braiman, R. Shainsky, and Y. Imry, Microwave-induced devil's staircase structure and chaotic behavior in current-fed Josephson junctions, Appl. Phys. Lett. **38**, 822 (1981).

[105] C. Reichhardt and F. Nori, Phase Locking, Devil's Staircases, Farey Trees, and Arnold Tongues in Driven Vortex Lattices with Periodic Pinning, Phys. Rev. Lett. **82**, 414 (1999).

[106] S.-B. Shim, M. Imboden, and P. Mohanty, Synchronized oscillation in coupled nanomechanical oscillators, Science **316**, 95 (2007).

[107] D. Z. Anderson, V. Mizrahi, T. Erdogan, and A. E. White, Production of in-fibre gratings using a diffractive optical element, Electron. Lett. **29**, 566 (1993).

[108] T. Antoni, K. Makles, R. Braive, T. Briant, P.-F. Cohadon, I. Sagnes, I. Robert-Philip, and A. Heidmann, Nonlinear mechanics with suspended nanomembranes, Europhys. Lett. **100**, 68005 (2012).

[109] L. S. Cutler and C. L. Searle, Some aspects of the theory and measurement of frequency fluctuations in frequency standards, Proc. IEEE **54**, 136 (1966).

[110] M. Dykman, X. Chu, and J. Ross, Stationary probability distribution near stable limit cycles far from Hopf bifurcation points, Phys. Rev. E **48**, 1646 (1993).

[111] B. Yurke and E. Buks, Performance of cavity-parametric amplifiers, employing Kerr nonlinearities, in the presence of two-photon loss, J. Lightwave Technol. **24**, 5054 (2006).

[112] S. Zaitsev, O. Shtempluck, E. Buks, and O. Gottlieb, Nonlinear damping in a micromechanical oscillator, Nonlinear Dyn. **67**, 859 (2012).

[113] Hannes Risken, *The Fokker-Planck Equation: Methods of Solution and Applications* (Springer, New York, 1996).

[114] K. Y. Fong, M. Poot, X. Han, and H. X. Tang, Phase noise of self-sustained optomechanical oscillators, Phys. Rev. A **90**, 023825 (2014).